# PCA SIFT Segmentation Based CAD System for the Detection of Lumbar Disc Herniation in MRI Images

Mamona Mumtaz \*a, Munir Ahmad b, Mirza Rahmat Baig c, Zeeshan Rasheed Mirza d

- a,c Department of Physics, University of Lahore, Lahore, Pakistan
- bd Institute of Nuclear Medicine and Oncology (INMOL), Lahore, Pakistan
- \*Corresponding author Email: \* mamonamumtaz6@gmail.com

#### **Abstract**

Globally low back pain is a significant threat to public health; in most cases, it is the first symptom of a herniated disc. The main objective is to develop a computer-aided diagnostic (CAD) system for automatically detecting the lumbar herniated disc in MRI images by applying a new segmentation technique, i.e., PCA-SIFT. This study anticipates a novel detection algorithm for the CAD system. We compared our results with the radiologist report, who independently reviewed lumbar spine MRI images. By using the clinical data of 50 patients, our proposed CAD system achieves 90% accuracy with sensitivity and specificity of 46% and 97%. Moreover, the AUC value of the CAD system is 0.832, which is considered excellent and shows superiority over existing algorithms. This study demonstrates that a lumbar disc herniation CAD system supported by PCA-SIFT segmentation and SVM classifier can be trained successfully with high accuracy and shortest processing time without marked MRI images. It believes that our CAD system will assist clinicians and radiologists in raising working efficiency.

**Keywords:** Computer-aided diagnosis, PCA-SIFT segmentation, Lumbar herniated disc, Sagittal MRI spine view, SVM classifier

#### Introduction

Computer-aided diagnosis (CAD) frameworks have been drawing in numerous scientists in the different human organs, for example, utilizing MRI to identify different types of diseases and prostate malignancy (Raja'S, Corso, Chaudhary, & Dhillon, 2011). In medicinal services, for the detection of various kinds of conditions, the role of radiologists and radiological imaging processes are significant. Positron Emission tomography (PET), Computed Tomography (CT), Magnetic Resonance Imaging (MRI), Ultrasound, X-Ray, are the different types of techniques which have progressed throughout the decades and made the imaging methodology exceptionally proficient.

The improvement of these techniques in image processing with the help of different software tools and algorithms supported the advancement of imaging processing because of continuous interest in the performing the analysis of input images, continuing to create different image processing algorithms which can assist the process of diagnosis of diseases by the radiologist. The motivation behind selecting MRI images for analysis is that it provides such a significant number of favourable circumstances when contrasted with other imaging methods (Kumar & Chatteijee, 2016).

Low back pain (LBP) is a common chronic disease today, and it is deteriorating, mainly because of the maturing and expanding total populace. Many people with low back pain couldn't accurately distinguish the specific nociceptive wellspring of their aggravation. That is why most patients with intense back torment are treated in a way that isn't steady with the

best practice treatment rules. Lumbar torment disorder is the second reason for answering to a specialist. It's the idea that 15% of unlucky deficiencies from work come from torment at the storage compartment, which leads to out of work in individuals beneath the age of 45 years (Peulić, Joković, Šušteršič, Peulić, and Medicine, 2020). According to Miller (2018), something other than one person in ten worldwide experiences low back torment. It was the intention of 60.1 million inabilities in 2015, an expansion of 54% starting around 1990, with the most extreme development happening in low-income countries.

(Tauqeer, Amjad, Ahmed, & Gillani, 2018) conducted a study in Pakistan to find out the ratio of low back pain in bankers with sample data of 164 bankers aged 22 – 58 years. Their findings showed that the chances of occurrence of lower back pain were 52.4% in bankers, and it is more prevalent in males than females. According to (Nurul, Haslinda, Saidi, Shamsul, & Zailina, 2010), the frequency of low back pain is superior in more prosperous countries than in developing countries, i.e., 42% and 35%. The prevalence of lower back pain causes high levels of care utilization and disability. There is an alarming fact that 80% of thepopulation in the world experienced LBP (Rubin, 2007).

Anatomy of the human lumbar spine consists of 33 vertebrae, and these vertebrae are connected with discs. The most well-known strategies utilized for the perception of the spine are MRI and CT. A lumbar herniated disc is characterized as restricted prolapse of the plate material past the limits of the intervertebral circle space. As indicated by (Peulić, Joković, Šušteršič, Peulić, & Medicine, 2020), roughly 75 per cent of lumbar flexion and augmentations acted in the lumbosacral joint at the level L5-S1, 20 per cent at L4-L5, and the remaining 5 per cent at upper lumbar levels. In this manner, the lumbar plate herniation is limited in 90 per cent of cases to the lower two groups, with those at the L5-S1 level being twice as upper level. Most of the abnormalities in the lumbar spine were identified by the radiologist with the help of Magnetic Resonance Imaging (MRI) scans of the patients intended for further referring to the specialized doctors for their treatment. The radiologist uses both the axial and sagittal MRI images of a patient's lumbar spine for diagnosis (De Souza & Frank, 2001). Fig.1 shows the Axial and Sagittal MRI views of the human lumbar spine.

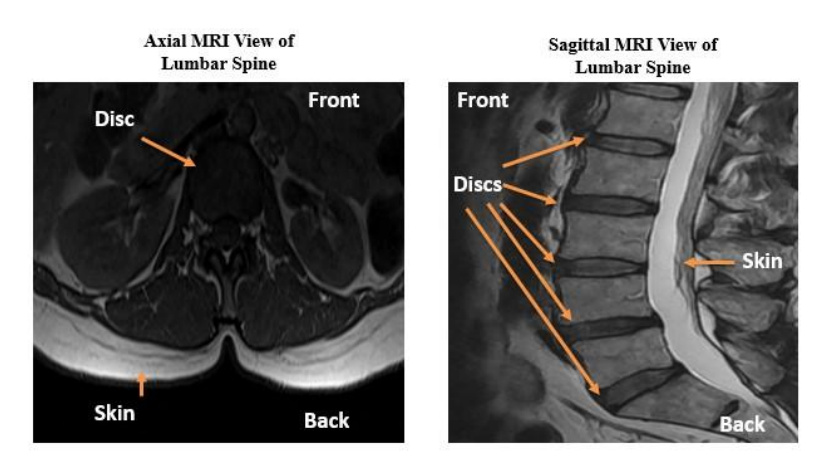


Fig. 1. Lumbar spine MRI images (Axial and Sagittal view)

Due to the incredible improvements in information technology and the handling of big data, the current approaches of detecting diseases from images using features or pattern recognitions make machine learning methods essential for data analysts. In the early 1970s,

imaging analysis for medical treatments was performed using different techniques, for example, fitting lines, region selection, circles and line and edge detectors. Later in the 1990s, these image analysis techniques became more popular in medical imaging (Litjens et al., 2017). Examples of these techniques are, Atlas methods and Active Shape Models (ASM) for image segmentation. The first CAD system was a mammography device developed by R2 Technology and approved by the Food and Drug Administration (FDA) of USA in 1998. Since that, the commercialization of CAD systems has continued in the diagnostic imaging field (Fujita & Technology, 2020).

CAD frameworks are mostly founded on picture preparation and dissecting the different patient information types to assist with accomplishing an exact determination. The reasoning behind building a CAD framework isn't to supplant but to help radiologists diagnose various illnesses. Hence, giving the radiologists clear and fast findings signs can work on radiologists' proficiency and may permit them to deal with more cases in a more limited period. Furthermore, incorporating the CAD framework into the determination cycle of different illnesses can work on numerous authoritative viewpoints, for example, creating clinical reports. At last, CAD frameworks give a superb stage to self-learning and education and may be utilized for research purposes (Al-Darabsah & Al-Ayyoub, 2013).

The remaining parts of this study are structured as follows, the next section briefly describes literature review on the CAD systems around the world that are currently used to detect different types of diseases. Section 3 defines the methodology section of this study and the basis of the planned CAD system for the detection of lumbar herniated discs. Finally, section 4 provides the results of this study and section 5 concludes the study with future work directions.

#### Literature Review

Due to the widespread lower back pain, mainly caused by the lumbar herniated disc that affects people's lives, the trend of detecting the disease with the help of computer-aided systems has become popular. Early in 1995, many efforts were made to discuss the methods for managing the lower back pain (Delitto, Erhard, & Bowling, 1995); (De Souza & Frank, 2001). This forum discusses different possibilities for the possible classifications of lower back pain. These types of methods helped develop a Computer-Aided Diagnostic system because of the central concept behind using an automatic procedure based on the set of features derived from the images.

Besides the enormous health problem, low back pain, mainly from the lumbar herniated disc, is also a financial issue that considerably troubles the government's well-being and social spending plan because of the distribution of clinical costs and installment for debilitated leave (Stephens & Bell, 1992). Albeit a few worldwide drives address the worldwide weight of low back torment as a general medical issue, there is a need to distinguish between financially savvy and setting explicit systems for overseeing low back torture to alleviate the results of the current and projected future weight.

Detection of different types of diseases or injuries in the body parts of humans in MRI images is the central part of diagnosing many diseases and the most challenging work for radiologists. Generally, the work comprises the localization and identification of the MRI images in some parts of the full images. Many researchers applied different CAD systems to detect the lumbar herniated disc through MRI images. Previously, the researchers have used a

high-resolution surface coil imaging technique for a lumbar herniated disk and found the comparison of computed tomography (Unal, Polat, Kocer, & Hariharan, 2015). By analyzing the data of 17 patients, they found that MRI is the best alternative for CT in detecting lumbar herniated discs (Edelman et al., 1985).

Currently, visual perception and examination of the lumbar spine MRI pictures is analyzed by diagnosing the lower back torment. This interaction could take up a remarkable radiologist's and doctor's time and exertion. Also, it can build the chance of misdiagnosis. In another sickness, a CAD framework were created to help the radiologists in the diagnosing system to act as an illustration of these frameworks, CAD framework for recognizing colonic polyp, CAD framework for distinguishing bosom malignant growth in mammography and CAD framework for identifying prostate disease utilizing MR pictures (Raja'S, Corso, Chaudhary, & Dhillon, 2010); (Taher, Werghi, & Al-Ahmad, 2015); (Arimura, Magome, Yamashita, & Yamamoto, 2009). Recently (Al-Ayyoub et al., 2018), proposed a CAD system that was based on SIFT-based Region of Interest (ROI) features to detect lumbar herniated discs in MRI.

## Methodology

This study proposed a CAD system that detects the lumbar disc herniation from sagittal MRI images of patients. Most of the tools and techniques used in this CAD system are implemented using MATLAB software. The details of patient data used in our CAD system and proposed methodology are as follows.

#### **Patients**

The local ethics committee approved our retrospective study (Reference number: INMOL/PA/2019). We performed retrospective research in the INMOL hospital (Institute of Nuclear Medicine & Oncology Lahore, Pakistan) for lumbar herniated disc patients that underwent an MRI examination of the hospital MRI scanners between January 2017 and October 2017. All 50 patients that met the inclusion criteria were included in our study, and there were no exclusions.

# Data and image acquisition

The MRI examinations were performed using a magnetic field 1.5 T. The dataset was in the original form of DCOM images. The sample data contains 38 patients' detailed attributes, i.e., patient sex, patient weight and age, and Echo time, etc. Signa HDxt of manufacturer GE Medical Systems scanner was used to extract MRI images of patients in a computer system. Scanning was performed with 3157 Repetition Time (TR), 100 Echo Time (TE), and a Flip Angle of 90. The radiologist with vast experience (Head, Radiology, INMOL) reviewed all the data images thoroughly and gave his opinion for training and testing datasets.

# **PCA-SIFT segmentation**

Our CAD system based on MATLAB GUI uses the PCA-SIFT segmentation technique, an automatic segmentation technique for feature extraction. Manual segmentation has many drawbacks; therefore, automatic segmentation mechanisms are preferable, and this area delivers an active research contribution (Duncan, Ayache, & intelligence, 2000). Automated segmentation methods provide better output results and are categorized by supervised or unsupervised methods (Bezdek, Hall, & Clarke, 1993). Generally, an unsupervised method of segmentation demands operator involvement only after the whole segmentation process is

complete, whereas the supervised methods need its operator interaction throughout the entire segmentation process. Thus, unsupervised segmentation methods are desirable for researchers to produce significant results. However, there are some cases where operator involvement is still required, such as error correction for unsatisfactory results (Clarke et al., 1995); (Olabarriaga & Smeulders, 2001).

PCA-SIFT segmentation system is a segmentation technique that acknowledges indistinguishable contributions from the standard SIFT (Scale Invariant Feature Transform) descriptor. (Lowe, 2004) exhibited SIFT calculations for separating distinctive invariant highlights from the images. It is broadly utilized in images mosaic, acknowledgment, and recovery, and so on. The filter consists of four phases: extreme recognition, purpose limitation, direction task, and descriptor. Principal Component Analysis (PCA) is a method for dimensionality reduction, which is appropriate to speak to the key point's patches and empower us to straightly extend high dimensional examples into a low dimensional component space (Nguyen, Forbes, & LJK).

#### **Features Extraction**

Literature survey shows that there are several methods available for the extraction of features from MRI images of the lumbar spine, the most popular is the Gray Level Co-occurrence Matrix (GLCM), method, in which parameters of input images are analyzed by the extraction of its feature parameters, for example, Mean, SD, RMS, Correlation, Energy, Variance, Entropy, Kurtosis, IDM, Contrast, Homogeneity and Skewness. GLCM of an image is characterized by a 2D matrix where each element has the probability of occurrence at intensity levels i and k (Prasad & Krishna, 2012); (Gebejes & Huertas, 2013); (Qurat-Ul-Ain, Kazmi, Jaffar, Mirza, & bases, 2010). The details of feature parameters are as follows.

#### Mean

Mean is the average value of the gray level intensities of the disc MRI image and can be calculated using equation 1.

$$\mu = \ \Sigma_{i=0}^{G-1} \quad i * p(i) \ ... \eqno(1)$$

Standard deviation (SD)

SD is the measure of the difference of image properties from its mean value. It describes the dispersion within a local region and is calculated using the formula in equation 2.

$$SD = \sqrt{\frac{1}{N-1} \sum_{i=0} (|Gi - \mu|^2)} ...$$
 (2)

# Entropy

It is the statistical measure of randomness and can be used to characterize the texture of the input image. Entropy is the evaluation parameter for disorders and can also be used to describe variation in the region. Entropy is calculated using the formula in equation 3.

$$E = -\sum_{i k} (p(i, k) \log \log (p(i, k))) \qquad (3)$$

## Root mean square (RMS)

RMS is frequently used to measure the differences between values predicted by the model and observed values. It computes values of each row or column of the input image along the entire input image using the formula in equation 4.

$$RMS = \sqrt{\frac{\sum_{i=1}^{M} |\mu_{i k}|^2}{M}}$$
 (4)

#### Variance

Variance is the intensity variation of the gray levels of the image and square root of the standard deviation and is calculated using the formula in equation 5.

$$\sigma^2 = \sum_{i=0}^{G-1} ((1-\mu)^2) p(i)$$
 .....(5)

#### **Smoothness**

Smoothness S is a measure of the gray level contrast used to establish the descriptors of relative smoothness and is determined using the formula in equation 6.

$$S = 1 - \frac{1}{1 + \sigma^2}$$
 (6)

#### **Kurtosis**

It measures the flatness of the distribution of gray histogram levels relative to a normal distribution. Kurtosis can be determined using the formula in equation 7.

$$k = [\sigma^{-4} \sum_{i=0}^{G-1} (1 - \mu)^4 p(i)] - 3$$
 (7)

#### **Skewness**

Skewness is the degree of asymmetry of pixel distribution in the specified window around its mean. It is the pure number that characterizes only the shape of the distribution and is calculated using equation 8.

$$S = \sigma^{-3} \sum_{i=0}^{G-1} (1 - \mu)^3 p(i)$$
 (8)

## **Inverse difference moment (IDM)**

IDM calculates the local homogeneity of the image and is similar to correlation. IDM is the measure of image texture and ranges from 0.0 to 1. IDM is calculated using the formula in equation 9.

$$IDM = \frac{p(i,k)}{[1+(i-k)*2]}...$$
(9)

## Contrast

Contrast is the localized gray level variation in the GLCM and is the feature its neighboring pixels are linearly dependent gray levels. It returns a measure of intensity contrast between the pixel and its neighbor over the whole image. Contrast is calculated using the formula in equation 10.

$$C = \sum_{ik} (|1 - k|^2) p(i, k)$$
 (10)

#### Correlation

Correlation is the measure of the gray level dependencies of the gray image. It measures how correlated a pixel is to its neighbor over the whole image. Correlation ranges from -1 to +1, and the +1 value indicates a perfect positive correlation, and -1 indicates a perfect negative correlation. It is calculated using equation 11.

$$\rho = \frac{1}{G-1} \tag{11}$$

## **Energy**

Energy is the opposite of entropy and determines the local homogeneity—the range of energy id 0 to 1, where 1 is for the constant image. Energy is calculated using equation 12.

$$E = \sum_{ik} p(i, k)^2$$
 (12)

## Homogeneity

Homogeneity is the inverse of contrast, and it measures of uniformity of non-zero entries of GLCM. The range of homogeneity is between 0 to 1, and 1 shows a diagonal GLCM.

$$H = \sum_{ik} \left( \frac{1}{|1 - (1 - k)^2|} \right) * p(i, k)$$
 (13)

## Classification

The classification technique used in our CAD system is the Support Vector Machine (SVM) classifier. Image classification process aims to categorize each disc feature using PCA-SIFT segmentation and find whether the disc is herniated or normal. The idea of the SVM classifier was presented in the early 90s. Today, its applications are found in many fields such as handwritten character recognition, time series prediction, data mining, medical diagnostics, bioinformatics, face detection, biomedical signal analysis, and image classification (Qurat-Ul-Ain et al., 2010).

## **Results and Findings**

To achieve our proposed CAD system results, we planned and developed an algorithm in the MATLAB software environment to classify the normal and herniated disc from a dataset of 50 patients. The CAD system is developed in GUI form in order to facilitate its user, as shown in figure 2. Since input MRI images are in the form of DICOM format, therefore, first we convert it into a suitable JPEG format. The CAD system as shown in figure 2 consists of inputs images and outputs images of GUI. The inputs CAD system (Load MRI Image, PCA SIFT Segmentation, and Classification Result) are programmed in MATLAB as pushbuttons. The outcomes of the system are shown in display panels that include the feature parameters of MRI images. Figure 3 to 5 shows the demo of loading images into the CAD system and obtaining results. In figure 3, we first have to load the image into the CAD system by clicking the Load MRI Image button. When the image is successfully loaded, the next step is to segment the input image using PCA SIFT segmentation by clinking the PCA SIFT Segmentation button; the procedure is shown in figure 4. As the CAD system segment the input image, its feature parameters (Mean, SD, Entropy, RMS, Variance, Smoothness, Kurtosis, Skewness, IDM, Contrast, Correlation, Energy, and Homogeneity) will be in display panel. Finally, figure 5 shows the results of the SVM classification of PCA SIFT segmented image in the form of "Normal" and "Herniated Disc".

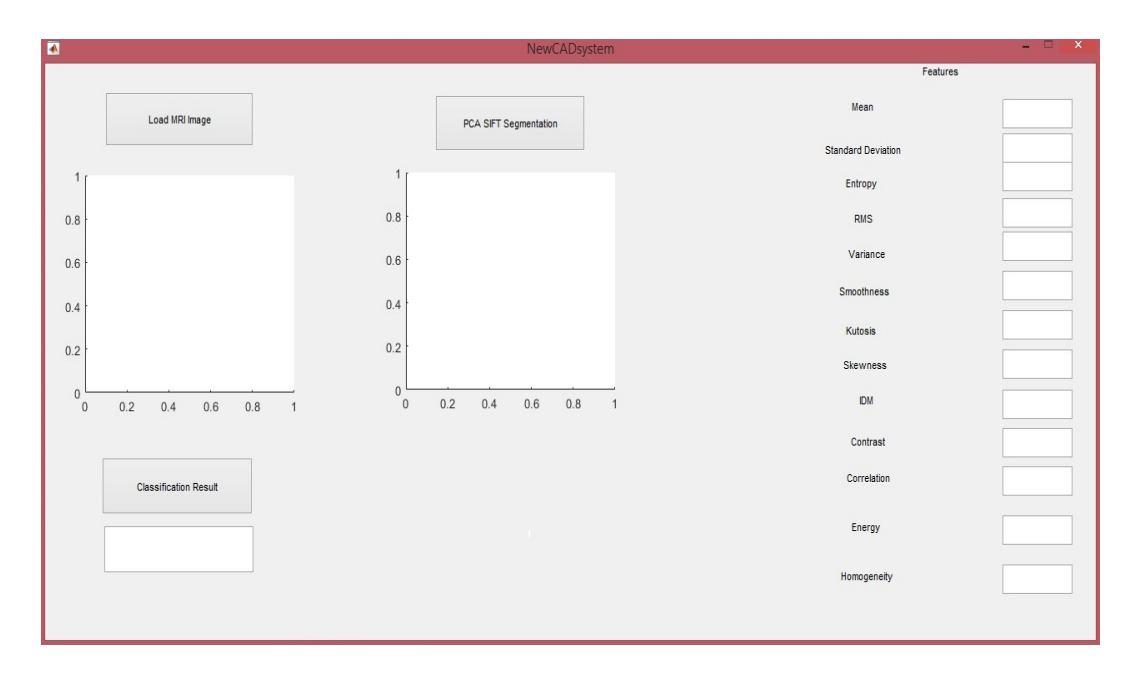


Fig. 2. Overview of CAD system

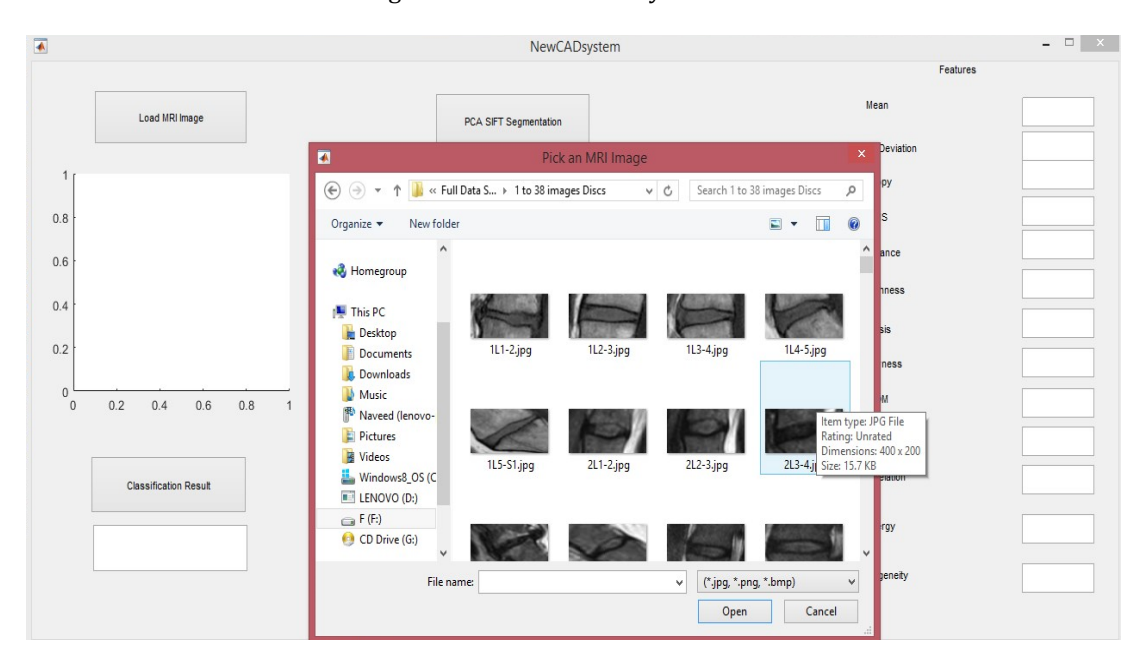


Fig. 3. Loading image in CAD system



Fig. 4. Segmentation and feature extraction in CAD system

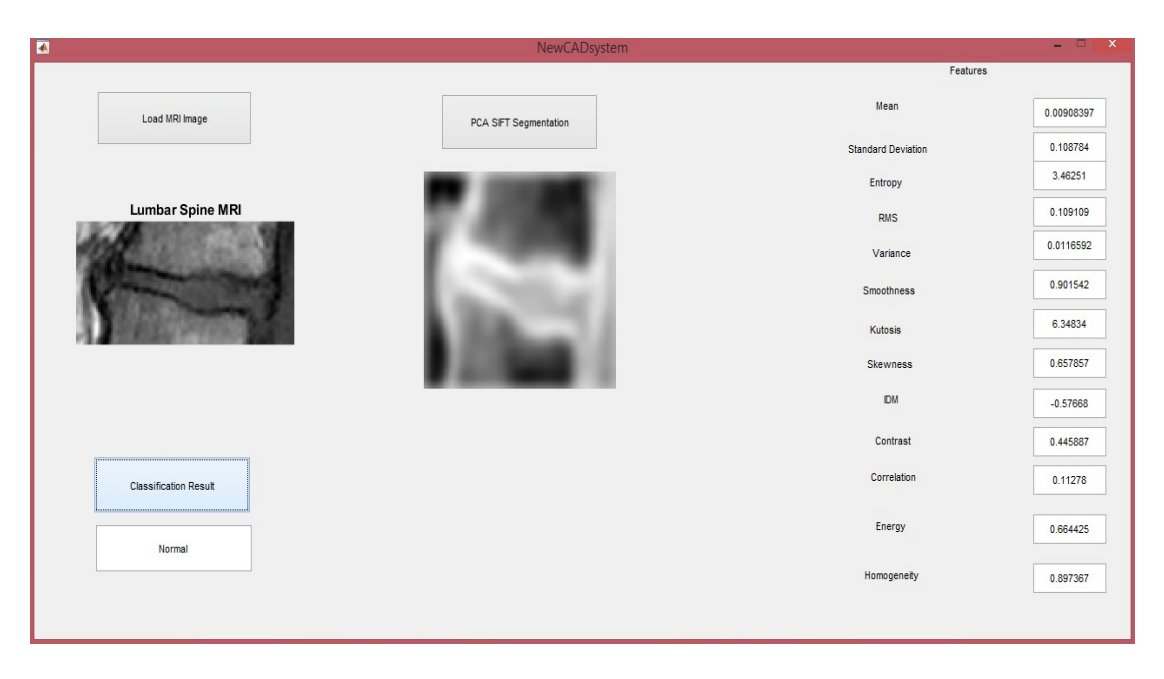


Fig. 5. Classification of the normal and herniated disc in the CAD system

The results of features extraction of 50 patient datasets are displayed in table 1. Table 1 shows no substantial differences in the GLCM values, except for few values where some value increases them compared to parameter values of other images. We can see that average features of Mean, Standard Deviation, Entropy, RMS, Variance, Skewness, IDM, and Contrast of normal disc are higher than a herniated disc. In comparison, the average feature values of Kurtosis, Energy, Correlation, and Homogeneity of a herniated disc are higher than normal disc.

Table 1. Results of GLCM features of PCA SIFT segmented images of normal and herniated discs

Features	Normal		Herniated	
1 Catalos	Average	Standard Deviation	Average	Standard Deviation
Mean	0.01806	0.10639	0.00271	0.00061
S.D	0.08891	0.02776	0.06676	0.00002
Entropy	1.84176	0.95089	1.76886	0.55345
RMS	0.08914	0.02798	0.06682	0.00000
Variance	0.01008	0.01386	0.00446	0.00001
Smoothness	0.91504	0.04379	0.94531	0.01321
Kurtosis	32.59068	29.19811	32.86011	14.33911
Skewness	3.14866	3.14134	2.33538	1.04929
IDM	2.39130	4.34703	0.10785	0.48243
Contrast	0.51235	0.47841	0.19103	0.04254
Correlation	0.12291	0.07347	0.13696	0.04296
Energy	0.85026	0.11040	0.89451	0.01960
Homogeneit y	0.95471	0.02681	0.96972	0.00454

Figure 6 to 9 shows the comparison GLCM features comparison of normal and herniated disc images graphically. Figure 6 displays the comparison of Mean and Standard Deviation of normal and herniated disc images. We can see that the normal disc features are normally distributed while herniated disc features are scattered on the left side of the graph. Similarly, figures 7 to 9 clearly show the difference between features (Contrast and Correlation, Energy and Homogeneity, Smoothness and Homogeneity) of a normal and herniated disc.

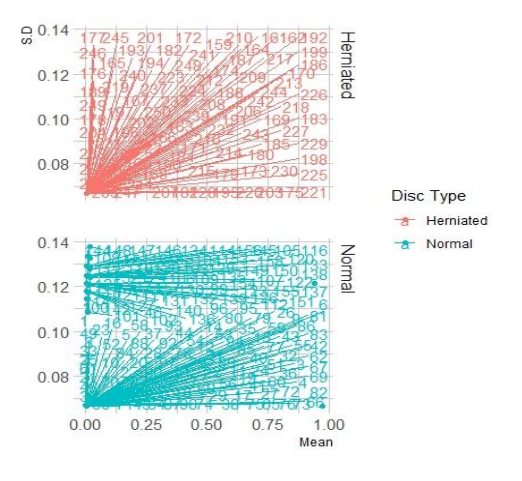


Fig. 6. Mean, and standard deviation features comparison of normal and herniated disc

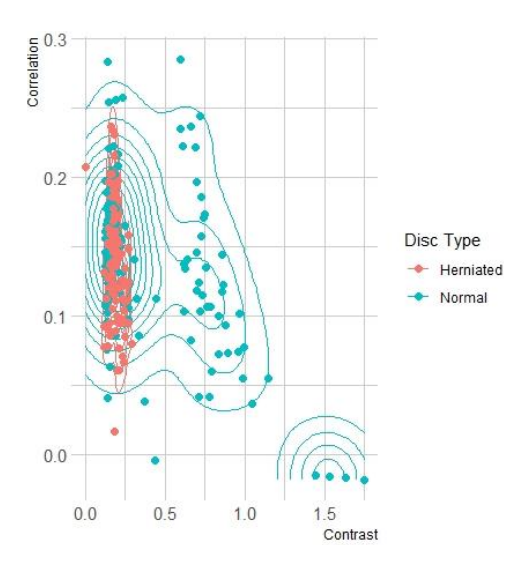


Fig. 7. Contrast and correlation features comparison of a normal and herniated disc

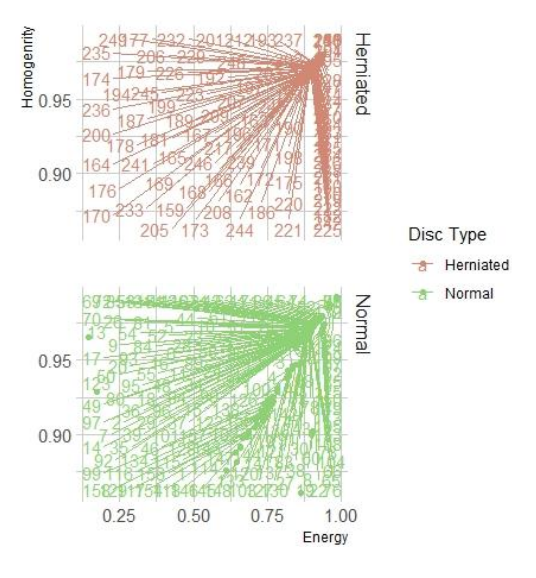


Fig. 8. Energy and Homogeneity features comparison of a normal and herniated disc

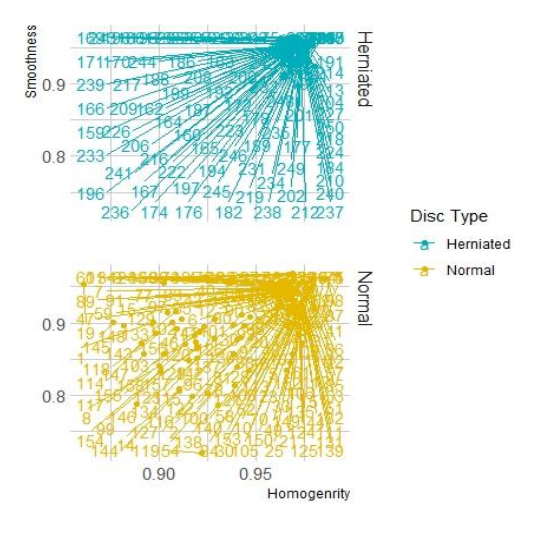


Fig. 9. Homogeneity and smoothness features comparison of a normal and herniated disc

Table 2 shows the analysis of the SVM classifier in terms of accuracy, sensitivity, specificity, predictive positive and negative parameters. The accuracy of the classifier is calculated using equation 14.

Accuracy<sub>i</sub> = 
$$\left(1 - \frac{1}{K} \sum_{j=1}^{K} |g_{ij} - n_{ij}|\right) \times 100\%$$
 (14)

Where Accuracy i = denotes classification accuracy at disc level i and  $1 \le I \le 5$ . Value of K denotes the number of cases in each testing, and g i j is the gold standard binary assignment for disc i and n i j is the resulting binary assignment for disc i from the inference in the model. Hence g i and n i are assigned the binary values the same way such that:

$$g_i = \begin{cases} 0 & \text{if disc } i \text{ is normal} \\ 1 & \text{if disc } i \text{ is abnormal} \end{cases}$$
 (15)

We compute the accuracy at each level independently to show the detailed classification accuracy at each level. In this way, we have more comprehension of the circle levels and their effect on classification accuracy. We acquire the clinical determination report for each case that contains a finding at each lumbar plate level. These reports are created by understanding inside our communitarian radiology focus. We think about these reports as the gold standard. The overall accuracy of our CAD system is 90%.

Table 2. Analysis of the SVM classifier for proposed CAD system

Analysis for Classifier							
Accuracy	Sensitivity	Specificity	Positive predictive	Negative predictive			
90%	46%	97%	91%	74%			

To calculate the sensitivity and specificity parameters of the CAD system, we use equations 16 to 19. The results in table 2 show that the SVM classifier has 46% sensitivity, 97% specificity, 91% positive predictive, and 74% negative predictive values for the proposed CAD system. The sensitivity results reflect that the probability of screening tests will be positive among those who are diseases. In contrast, the specificity test reflects the probability that the screening test will be negative among those who don't have the condition. The lower sensitivity and higher specificity indicate that normal cases are more than the herniated cases in the sample data. Thus sensitivity and specificity also help determine the type of disc, whether it is normal or herniated.

Specificity = 
$$\frac{TN}{TN+FP}$$
 (16)

Sensitivity = 
$$\frac{TP}{TP+FN}$$
....(17)

Predictive value positive = 
$$\frac{TP}{TP+FP}$$
 .... (18)

Predictive value negative = 
$$\frac{TN}{TN+FN}$$
 (19)

Figure 10 shows the Receiver Operating Characteristic (ROC) bend of affectability and explicitness of our CAD framework. ROC diagram is a plot of all affectability and explicitness sets coming about because of ceaselessly changing the choice edge over the whole scope of results noticed. For each situation, the ROC plot portrays the cross-over between the two appropriations by plotting the affectability versus 1-particularity for the total scope of choice edges. The region under the bend (AUC) of the ROC bend is 0.832. A ROC bend can be viewed as the normal worth of the affectability for a test over all conceivable particularity esteems or the other way around. AUC is a successful way of summing up the in general indicative precision of the test. It takes 0 to 1, where a worth of 0 shows a totally erroneous test and a worth of 1 mirrors a completely exact test. The AUC worth of our CAD framework is 0.832, which is adequate and considered magnificent (Mandrekar, 2010). Additionally, figure 11 shows the genuine positive, genuine negative, bogus positive, and bogus negative cases graphically.

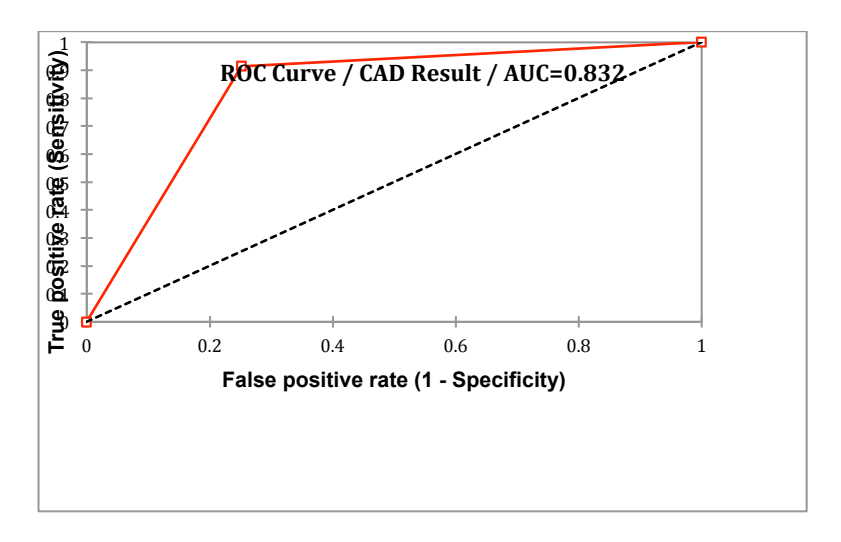


Fig. 10. ROC curve of sensitivity and specificity

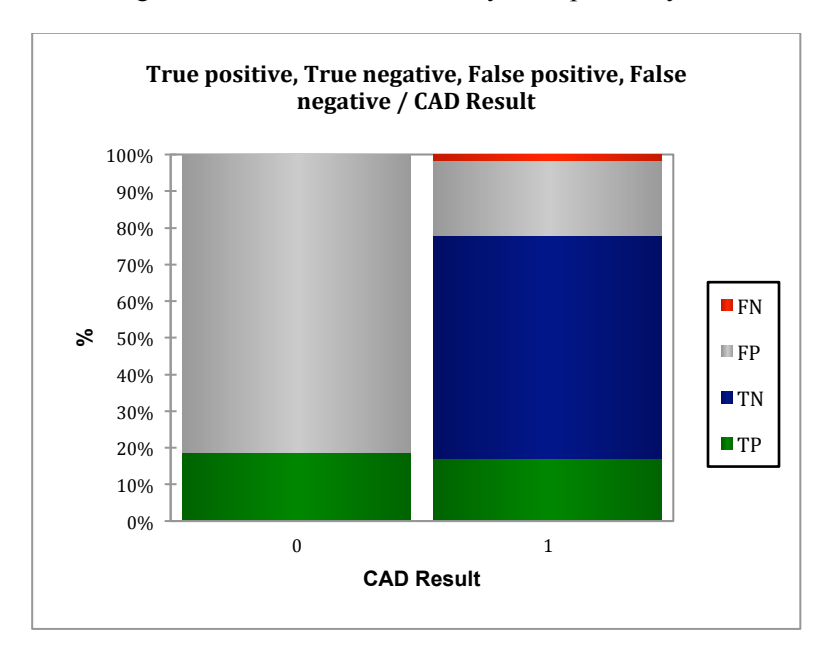


Fig. 11. Graph of true positive, true negative, false positive and false negative

## **Conclusion**

The radiologists' explanation of MRI images is complicated, even for experienced radiologists (Bellotti et al., 2006). From this point of view, the proposed CAD system can be a valuable tool to help them. We proposed an innovative PCA-SIFT segmentation-based CAD system to detect lumbar herniated disc from MRI images of patients. Using the clinical data of 50 patients, the disc images were analyzed and segmented using PCA-SIFT segmentation technique, and different features were extracted. Based on extracted features, the SVM classifier classifies the discs into two categories, i.e., Normal and Herniated. The proposed CAD system achieves the accuracy of 90%. The sensitivity and specificity of the CAD system are 46% and 97%. The AUC value of the CAD system is 0.832, which is considered excellent. Findings indicate that even the proposed methodology is simple as compared with the previous methods available in CAD systems, the accuracy is precise, and many enhancements are still possible in this CAD system. The probable improvement may be applied carefully for selecting the possible features to be included in the CAD system for the purpose of detecting the herniated disc in MRI images. In future work future work, we may applied other images classification techniques and may also reduce the GUI interface regarding window size and moving steps. We may apply these enhancements in our CAD system in our future study.

#### References

- Al-Ayyoub, M., Al-Mnayyis, N., Alsmirat, M. A., Alawneh, K., Jararweh, Y., Gupta, B. B. J. J. o. A. I., & Computing, H. (2018). SIFT based ROI extraction for lumbar disk herniation CAD system from MRI axial scans. 1-9.
- Al-Darabsah, K., & Al-Ayyoub, M. (2013). *Breast cancer diagnosis using machine learning based on statistical and texture features extraction.* Paper presented at the Proceedings of the 4th International conference on information and communication systems (ICICS 2013).
- Arimura, H., Magome, T., Yamashita, Y., & Yamamoto, D. J. A. (2009). Computer-aided diagnosis systems for brain diseases in magnetic resonance images. 2(3), 925-952.
- Bellotti, R., De Carlo, F., Tangaro, S., Gargano, G., Maggipinto, G., Castellano, M., . . . Magro, R. J. M. p. (2006). A completely automated CAD system for mass detection in a large mammographic database. *33*(8), 3066-3075.
- Bezdek, J. C., Hall, L., & Clarke, L. P. J. M. P.-L. P.-. (1993). Review of MR image segmentation techniques using pattern recognition. *20*, 1033-1033.
- Clarke, L., Velthuizen, R., Camacho, M., Heine, J., Vaidyanathan, M., Hall, L., . . . Silbiger, M. J. M. r. i. (1995). MRI segmentation: methods and applications. *13*(3), 343-368.
- De Souza, L., & Frank, A. (2001). Conservative management of low back pain.
- Delitto, A., Erhard, R. E., & Bowling, R. W. J. P. t. (1995). A treatment-based classification approach to low back syndrome: identifying and staging patients for conservative treatment. 75(6), 470-485.
- Duncan, J. S., Ayache, N. J. I. t. o. p. a., & intelligence, m. (2000). Medical image analysis: Progress over two decades and the challenges ahead. 22(1), 85-106.
- Edelman, R. R., Shoukimas, G. M., Stark, D. D., Davis, K. R., New, P., Saini, S., . . . Brady, T. J. J. A. j. o. r. (1985). High-resolution surface-coil imaging of lumbar disk disease. *144*(6), 1123-1129
- Fujita, H. J. R. P., & Technology. (2020). AI-based computer-aided diagnosis (AI-CAD): the latest review to read first. *13*(1), 6-19.
- Gebejes, A., & Huertas, R. J. d. (2013). Texture characterization based on grey-level co-occurrence matrix. 9, 10.
- Kumar, P. S., & Chatteijee, S. (2016). Computer aided diagnostic for cancer detection using MRI images of brain (Brain tumor detection and classification system). Paper presented at the 2016 IEEE Annual India Conference (INDICON).
- Litjens, G., Kooi, T., Bejnordi, B. E., Setio, A. A. A., Ciompi, F., Ghafoorian, M., . . . Sánchez, C. I. J. M. i. a. (2017). A survey on deep learning in medical image analysis. 42, 60-88.

- Lowe, D. G. J. I. j. o. c. v. (2004). Distinctive image features from scale-invariant keypoints. 60(2), 91-
- Mandrekar, J. N. J. J. o. T. O. (2010). Receiver operating characteristic curve in diagnostic test assessment. *5*(9), 1315-1316.
- Nguyen, H., Forbes, F., & LJK, M. Multivariate exponential family principal component analysis.
- Nurul, I., Haslinda, A., Saidi, M., Shamsul, B., & Zailina, H. J. A. J. o. A. S. (2010). Prevalence of low back pain and its risk factors among school teachers. 7(5), 634-639.
- Olabarriaga, S. D., & Smeulders, A. W. J. M. i. a. (2001). Interaction in the segmentation of medical images: A survey. 5(2), 127-142.
- Peulić, M., Joković, M., Šušteršič, T., Peulić, A. J. C., & Medicine, M. M. i. (2020). A Noninvasive Assistant System in Diagnosis of Lumbar Disc Herniation. *2020*.
- Prasad, B., & Krishna, A. (2012). *Classification of medical images using data mining techniques*. Paper presented at the International Conference on Advances in Communication, Network, and Computing.
- Qurat-Ul-Ain, G. L., Kazmi, S. B., Jaffar, M. A., Mirza, A. M. J. R. a. i. a. i., knowledge engineering, & bases, d. (2010). Classification and segmentation of brain tumor using texture analysis. 147-155
- Raja'S, A., Corso, J. J., Chaudhary, V., & Dhillon, G. (2010). *Automatic diagnosis of lumbar disc herniation with shape and appearance features from MRI*. Paper presented at the Medical Imaging 2010: Computer-Aided Diagnosis.
- Raja'S, A., Corso, J. J., Chaudhary, V., & Dhillon, G. (2011). Toward a clinical lumbar CAD: herniation diagnosis. *International journal of computer assisted radiology and surgery*, 6(1), 119-126
- Rubin, D. I. J. N. c. (2007). Epidemiology and risk factors for spine pain. 25(2), 353-371.
- Stephens, S. E., & Bell, G. R. J. L. D. D., RW Hardy, Ed. (1992). Natural history and epidemiology of lumbar disc degeneration. 13-15.
- Taher, F., Werghi, N., & Al-Ahmad, H. J. A. (2015). Computer aided diagnosis system for early lung cancer detection. 8(4), 1088-1110.
- Tauqeer, S., Amjad, F., Ahmed, A., & Gillani, S. A. J. K. M. U. J. (2018). PREVALENCE OF LOW BACK PAIN AMONG BANKERS OF LAHORE, PAKISTAN. 10(2).
- Unal, Y., Polat, K., Kocer, H. E., & Hariharan, M. J. A. S. C. (2015). Detection of abnormalities in lumbar discs from clinical lumbar MRI with hybrid models. *33*, 65-76.